NANO LETTERS

pubs.acs.org/NanoLett Letter

Combination of Physicochemical Tropism and Affinity Moiety Targeting of Lipid Nanoparticles Enhances Organ Targeting

Marco E. Zamora,[#] Serena Omo-Lamai,[#] Manthan N. Patel, Jichuan Wu, Evguenia Arguiri, Vladmir R. Muzykantov, Jacob W. Myerson,* Oscar A. Marcos-Contreras,* and Jacob S. Brenner*

Cite This: *Nano Lett.* 2024, 24, 4774−4784 Read Online

ACCESS | Metrics & More | Article Recommendations | Supporting Information

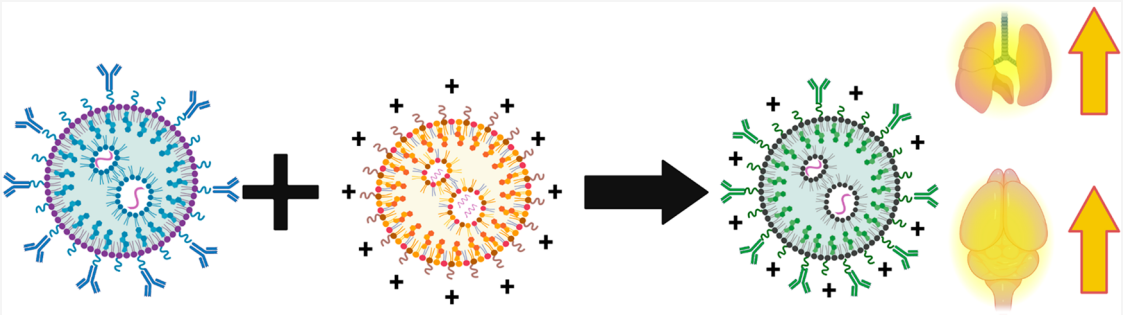

ABSTRACT: Two camps have emerged for targeting nanoparticles to specific organs and cell types: affinity moiety targeting and physicochemical tropism. Here we directly compare and combine both using intravenous (IV) lipid nanoparticles (LNPs) designed to target the lungs. We utilized PECAM antibodies as affinity moieties and cationic lipids for physicochemical tropism. These methods yield nearly identical lung uptake, but aPECAM LNPs show higher endothelial specificity. LNPs combining these targeting methods had >2-fold higher lung uptake than either method alone and markedly enhanced epithelial uptake. To determine if lung uptake is because the lungs are the first organ downstream of IV injection, we compared IV vs intra-arterial (IA) injection into the carotid artery, finding that IA combined-targeting LNPs achieve 35% of the injected dose per gram (%ID/g) in the first-pass organ, the brain, among the highest reported. Thus, combining the affinity moiety and physicochemical strategies provides benefits that neither targeting method achieves alone.

KEYWORDS: *extrahepatic delivery, physicochemical, antibody-mediated, lung targeting, cell-type expression*

Nanoparticles have held the promise of selectively targeting specific cell types and organs, though that goal has remained largely elusive for organs other than the liver, the natural clearance organ for intravenous nanoscale materials.[1−5] In working to achieve this targeting goal in nonliver organs, two strategies have predominated, termed here "affinity moiety targeting" and "physicochemical tropism".

"Affinity moiety targeting", developed first, employs "affinity moieties" that bind specifically to chosen epitopes on target cells, e.g., conjugating nanoparticles to monoclonal antibodies that have affinity for the target cell. First achieved by Torchilin and others, who showed the benefits of conjugating liposomes to monoclonal antibodies.[6−11] Numerous other affinity moieties have been used besides monoclonal antibodies, including small molecules that bind to receptors on target cells, aptamers, and antibody fragments (Fab, $F(ab')_2$, etc.).[12−21] At least 10 affinity-moiety-targeted nanoparticles have reached clinical studies, though none are approved.[19,22,23]

"Physicochemical tropism" utilizes nanoparticle physical properties (size, shape, and charge) or chemical features (binding to specific endogenous proteins because of the nanoparticles' chemical makeup) to effect organ tropism. In general, physicochemical tropism is not easy to design from first-principles, and therefore commonly achieved by screening libraries of nanoparticles with slightly varying formulations to find ones with tropism for a particular cell or organ, as exemplified by lipid nanoparticle (LNP) screens, especially Anderson's studies of the early 2010s.[24−27] These optimized searches through LNP formulation space have produced numerous formulations with physicochemical tropism for particular organs or cell types, ranging from the lungs to spleen, and achieving cell-type-specificity to macrophages and T-cells.[28−32] The first FDA-approved RNA-loaded lipid nanoparticle (LNP), patisiran, approved in 2018, has

Received: December 20, 2023
Revised: April 2, 2024
Accepted: April 3, 2024
Published: April 10, 2024

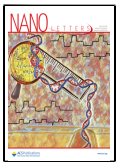

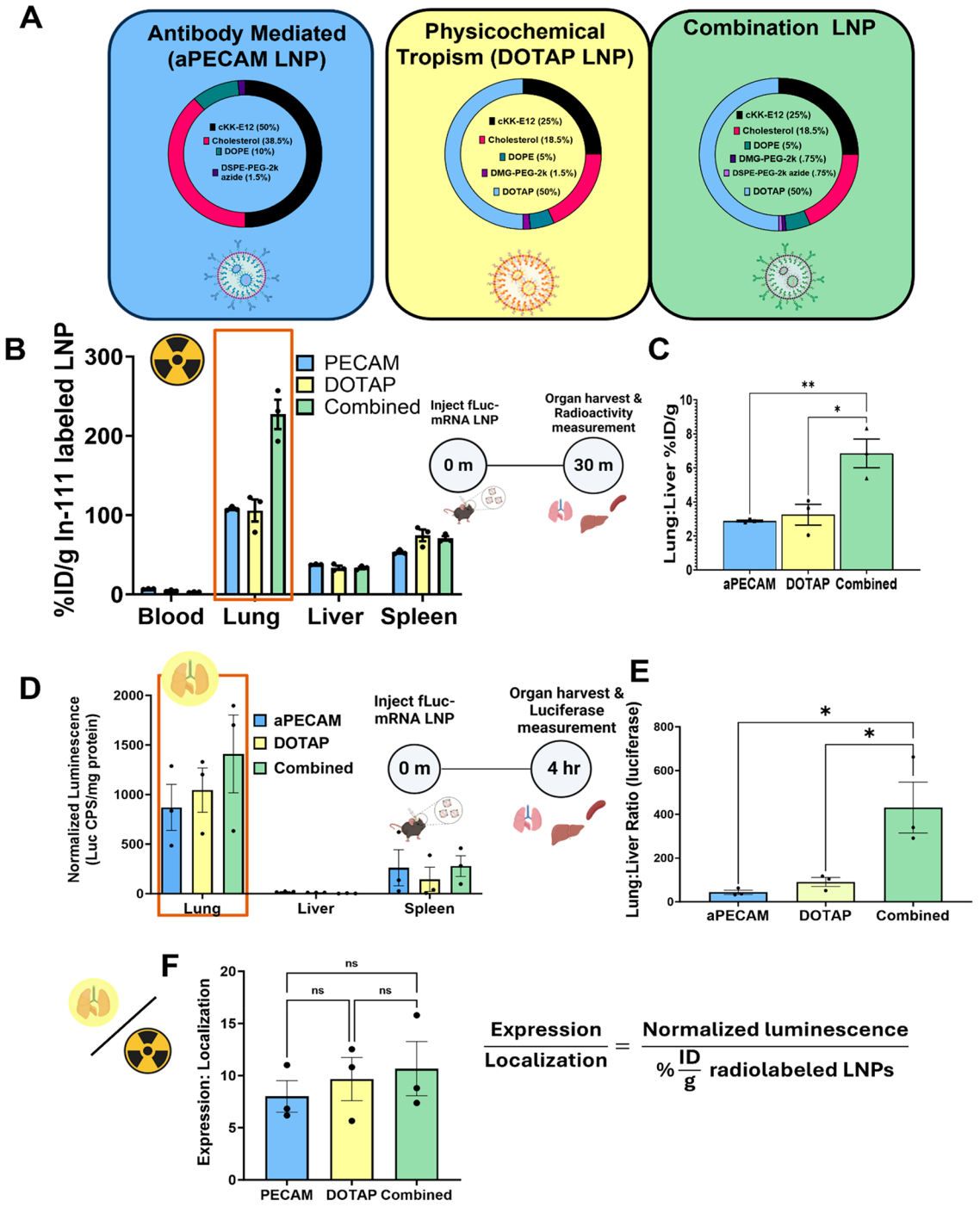

Figure 1. LNPs formulated with cationic lipids and targeted to PECAM show improved lung localization and expression. (A) Formulations and molar percentages of aPECAM, DOTAP, and Combined LNPs. (B) Biodistributions of aPECAM, DOTAP, and Combined LNPs 30 min after LNP injection. Combined LNPs localize to the lungs >2-fold more than aPECAM or DOTAP LNPs. (C) Lung-to-liver ratios obtained from (B) were calculated by dividing the %ID/g of tissue in the lung by that in the liver. Combined LNPs have a >2-fold higher lung-to-liver ratio compared to aPECAM or DOTAP LNPs. (D) Luciferase expression of aPECAM, DOTAP, and Combined LNPs in the lung, liver, and spleen 4 h after LNP injection. (E) Lung-to-liver ratios were calculated from (D) by dividing the normalized luciferase expression values in the lung by that in the liver. The lung-to-liver ratio of combined LNPs is about 10- and 5-fold higher than both aPECAM and DOTAP LNPs, respectively. (F) Ratios of lung expression to localization calculated by dividing the normalized luciferase expression values from (D) to the %ID/g of tissue values from (A) for each LNP formulation. The expression to localization ratios are not significantly different between formulations indicating a good correlation between LNP localization and luciferase mRNA expression. Statistics: $n = 3$ and data shown represent mean ± SEM. Comparisons between groups were made using 1-way ANOVA with Tukey's posthoc test. *$p < 0.05$, ***$p < 0.001$, ****$p < 0.0001$.

physicochemical tropism to the plasma protein ApoE, which selectively shuttles the LNPs to hepatocytes.[33]

Much has been written comparing affinity moiety targeting and physicochemical tropism.[24−32,34−44] Advantages cited for affinity moieties include a known mechanism of action, enabling rational engineering. Physicochemical targeting usually does not have a known mechanism of action (ApoE binding is a rare exception), and therefore, rational engineering

https://doi.org/10.1021/acs.nanolett.3c05031
Nano Lett. 2024, 24, 4774−4784

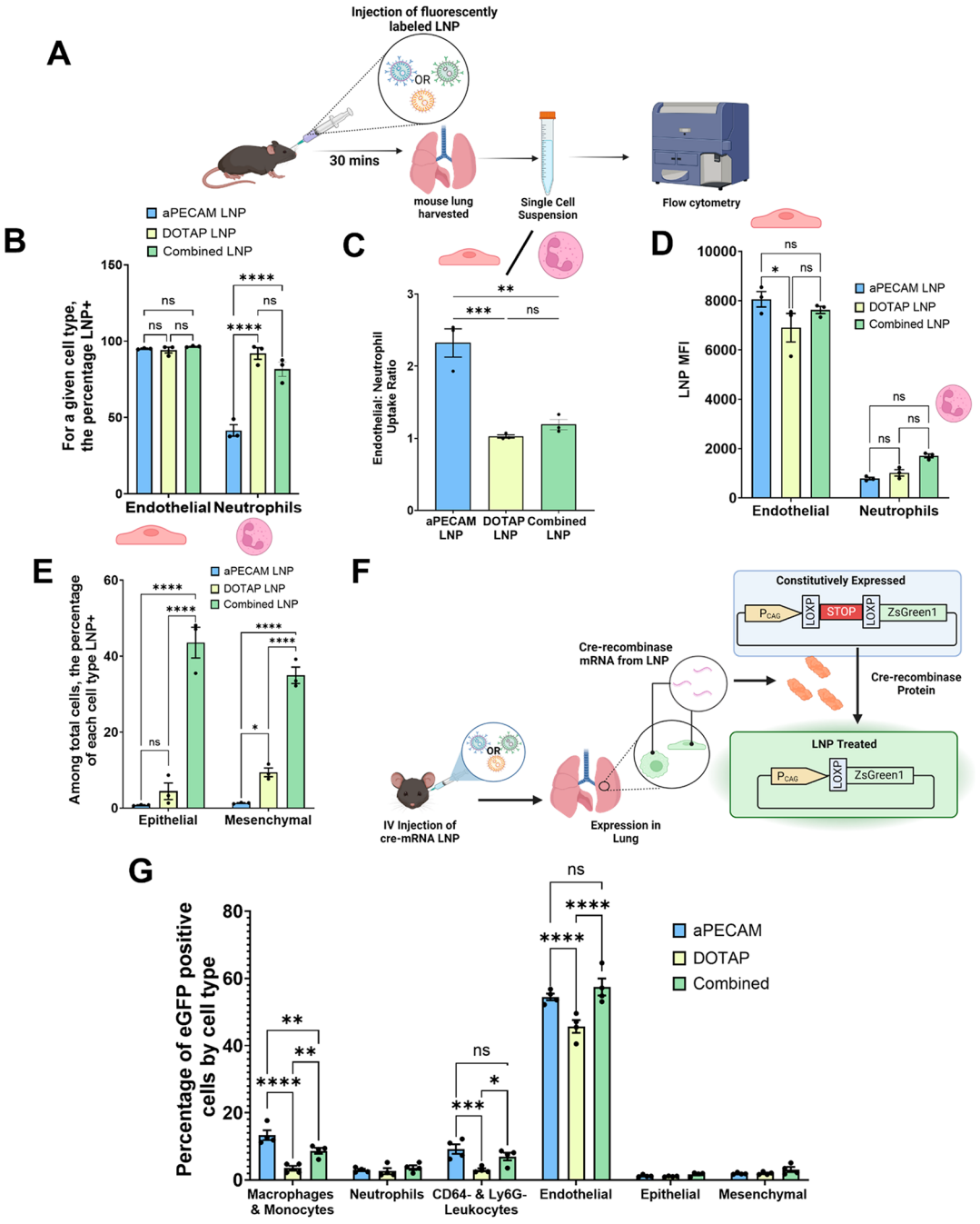

Figure 2. Combined LNPs have enhanced uptake in epithelial and mesenchymal cells in vivo in the lung, but also high uptake by neutrophils. (A) Schematic showing the flow cytometry protocol used, where fluorescently labeled aPECAM, DOTAP, or Combined LNPs were IV injected into mice at a dose of 7.5 μg of RNA, allowed to circulate for 30 min before being sacrificed, and the lungs were prepared as single-cell suspensions. (B) Gating first by cell type, e.g., endothelial cells and neutrophils, we then looked at the percentage of each cell type that was positive for aPECAM, DOTAP, or Combined LNPs. Data show enhanced neutrophil uptake of DOTAP and Combined LNPs. (C) Endothelial-to-neutrophil (E:N) uptake ratio of aPECAM, DOTAP, and Combined LNPs. Values greater than 1 indicate endothelial cell preference compared to neutrophils. aPECAM LNPs are shown to have higher endothelial preference. (D) LNP mean fluorescence intensity (MFI) for LNP formulations shows that while DOTAP and Combined LNPs have a lower E:N ratio compared to aPECAM LNPs, the endothelial cells that take up these LNPs do so highly and equally to aPECAM LNPs. (E) Gating first by cell type (as in B) and then plotting LNP positivity among epithelial and mesenchymal cells. These cells are further away from the vascular lumen than endothelial cells and neutrophils and generally harder to access via intravenous administration. DOTAP and, more so, Combined LNPs are able to cross and be taken up by these two cell types, with Combined LNPs achieving higher epithelial uptake than both DOTAP and aPECAM LNPs. (F) Schematic depicting Cre mRNA LNP-driven deletion of LoxP-flanked STOP cassette on Ai6 reporter mice to determine cell types that take up and express Cre-mRNA cargo. We inject aPECAM, DOTAP, or Combined LNPs via an intravenous route. After 24 h, mice were sacrificed and cell types assessed for enhanced GFP (eGFP) signal driven by the ZsGreen1 gene. (G) Using this method, we found that pulmonary endothelial cells had the highest rate of expressing eGFP. We observed that aPECAM and Combined LNPs outcompeted DOTAP LNPs for endothelial cell expression of eGFP. Statistics: $n = 3$ and data shown represents mean ± SEM. For Ai6 mouse experiments, a $n = 4$ was used and data are presented as mean ± SEM. Comparisons between groups were made using 1-way ANOVA or 2-way ANOVA with Tukey's posthoc test where appropriate. *$p < 0.05$, ***$p < 0.001$, ****$p < 0.0001$.

https://doi.org/10.1021/acs.nanolett.3c05031
Nano Lett. 2024, 24, 4774−4784

is difficult. However, physicochemical targeting has a large advantage for industrialization, as affinity moieties such as antibodies are not easy to conjugate to nanoparticles and purify at scale.[45,46] Physicochemical targeting, for LNPs at least, usually just involves changing the lipid formulation, which is facile at industrial scale.[47] Thus, each approach has relative advantages and disadvantages. These two approaches have rarely been tested head-to-head, especially for LNPs. This lack of head-to-head testing might be because in general these two approaches are performed in separate laboratories, falling into separate "camps."

Here, we directly compare cell and organ delivery efficiency and specificity when delivering to a single organ, the lung, using PECAM for affinity targeting vs cationic lipids for physicochemical targeting. We do this for LNPs, since they are the leading nanoparticle format currently under development in industry, with billions invested in the past few years.[48,49] We chose to target the lungs because many formulations with both affinity and physicochemical targeting have been created with the goal of ameliorating alveolar diseases, especially acute respiratory distress syndrome (ARDS), the alveolar inflammatory disease that was the primary cause of death during the COVID-19 pandemic and still causes >75000 deaths each year from non-COVID types of ARDS.[50−55]

For affinity-moiety targeting to the alveolar vasculature, we chose LNPs conjugated to antibodies against PECAM-1. Compared to untargeted LNPs, PECAM targeting has been shown to increase mRNA delivery and protein expression in the lung by ∼200- and 25-fold, respectively.[36] PECAM has been compared to other affinity moieties, and none performs markedly better with respect to lung uptake. For physicochemical tropism in the lungs, we chose LNPs incorporating a cationic lipid. Numerous LNPs have been formulated that have physicochemical tropism to the lungs, with the commonality that nearly all possess lipids bearing positive charges within biologically relevant pH ranges. Some of these are ionizable lipids with tertiary amines, while others are permanently cationic with quaternary amines.[28,30,56] Here we chose the most cited such LNP formulation, which includes DOTAP, a permanently cationic lipid with a quaternary amine,[28−30,57] shown to drive expression of mRNA-luciferase to the lungs.[28−30,57]

In a comparison of aPECAM and DOTAP LNPs, we find that they have nearly identical localization to the lungs, despite dramatically different targeting mechanisms. We then show that combining PECAM antibodies and DOTAP into a single LNP produces a synergistic benefit, achieving the highest reported delivery of an LNP to the lungs, suggesting that bringing together these two approaches can produce higher uptake than either alone.

To begin these studies, we chose the ionizable lipid cKK-E12 for our base formulation, which others in the field have shown drives high expression from mRNA cargo.[58−60] We formulated affinity-moiety-targeted LNPs by conjugating aPECAM antibodies to the LNP surface (herein referred to as "aPECAM LNPs"). We fabricated LNPs with physicochemical tropism to the lungs by adding a cationic lipid, DOTAP, as published previously (herein referred to as "DOTAP LNPs"). "Combined LNPs" were formulated by conjugating aPECAM antibody to the surface of DOTAP LNPs (Figure 1A). We added a radiotracer lipid (Indium-111-DTPA-PE) to the LNPs and intravenously (IV) injected them into healthy mice at a dose of 7.5 μg mRNA per mouse. After allowing the LNPs to circulate for 30 min, the amount of radioactivity in each organ was measured and recorded as the percent of injected dose per gram of tissue (%ID/g). We found that aPECAM and DOTAP LNPs achieved essentially identical lung uptake, despite different targeting mechanisms. LNPs combining the two targeting techniques localize to the lungs >2-fold more than either DOTAP or aPECAM LNPs (Figure 1B). Similarly, Combined LNPs have a >2-fold higher lung-to-liver localization ratio than aPECAM or DOTAP LNPs (Figure 1C).

To measure protein expression, we fabricated aPECAM, DOTAP, and Combined LNPs loaded with luciferase mRNA. LNPs were IV-injected into healthy mice, then sacrificed 4 h later for measurement of luciferase activity in each organ. Combined LNPs have a >2-fold and >1.6-fold higher luciferase expression in the lungs compared to aPECAM or DOTAP LNPs, respectively (Figure 1D). Combined LNPs also have 10-fold and 5-fold higher lung-to-liver luciferase expression ratios than aPECAM and DOTAP LNPs, respectively, (Figure 1E). Lung-expression-to-uptake ratios were obtained by dividing the normalized luciferase expression values in Figure 1E by the %ID/g values in Figure 1A (Figure 1F). We found no significant difference in the expression-to-uptake ratio between formulations, indicating that Combined LNPs' advantage in luciferase expression is due entirely to their improved lung localization (deposition of nanoparticles in the lung) rather than an advantage in the amount of luciferase expression produced by each LNP that stays in the lungs.

To investigate the different cell types that take up our three different LNP formulations, we used flow cytometry to trace fluorescent aPECAM, DOTAP, and combined LNPs in cells isolated from lungs 30 min after IV injection of the LNPs (Figure 2A; gating strategy shown in Supporting Figure 2). We determined the percentage of endothelial cells and neutrophils that take up our LNPs (Figure 2B). All three formulations achieve high uptake in endothelial cells (>85% of endothelial cells were LNP-positive) with no significant difference between them. Neutrophils took up DOTAP and Combined LNPs in significant quantities (90% and 80% of neutrophils were positive for DOTAP and Combined, respectively), whereas only 41% of neutrophils were positive for aPECAM LNPs. Endothelial-to-neutrophil uptake ratios (Figure 2C) show that aPECAM LNPs have clear endothelial preference compared to that of DOTAP and Combined LNPs. aPECAM and Combined LNPs had similar mean fluorescence intensities, with a small but significant edge to that of aPECAM LNPs over DOTAP LNPs (Figure 2D). A large fraction of neutrophils took up DOTAP and Combined LNPs, however, MFI data show that these LNPs were taken up in significantly greater concentrations by endothelial cells, compared to neutrophils. We assessed LNP uptake in alveolar mesenchymal and epithelial cells and cells further away from the alveolar capillary lumen (Figure 2E). DOTAP-containing LNPs can reach these deeper cell types.[28,29] aPECAM and DOTAP LNPs are taken up by <1% and 4% of epithelial cells, respectively. However, epithelial cells take up a staggering 40% of Combined LNPs. Similarly, mesenchymal cells take up 35% of the Combined formulation (Figure 2E). In summary, aPECAM LNPs are more endothelial-specific than DOTAP-containing LNPs, with DOTAP-containing LNPs being taken up by a high fraction of neutrophils but with only a moderate amount of uptake per cell, as compared to endothelial cells.

We assessed monocytes/macrophages and lymphocytes (Supporting Figure 3A,F). DOTAP and Combined LNPs

https://doi.org/10.1021/acs.nanolett.3c05031
Nano Lett. 2024, 24, 4774−4784

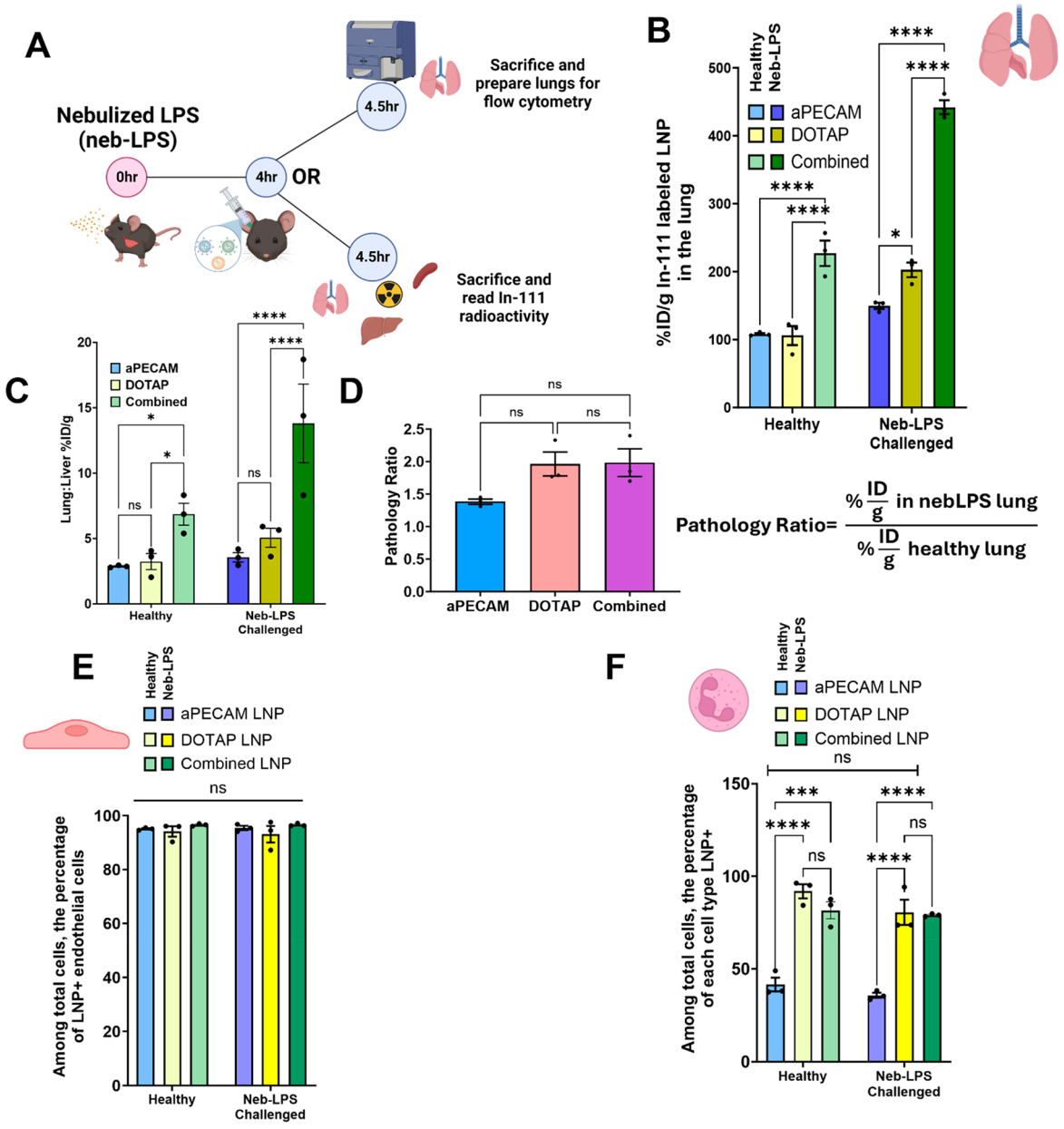

Figure 3. Combined LNPs show superior lung localization in a mouse model of acute lung inflammation. (A) Schematic of nebulized-LPS injury and resulting assays performed, briefly 4 h after neb-LPS injury, mice are either injected with fluorescently labeled or Indium-111 (In-111) radiolabeled nanoparticles, allowed to circulate for 30 min before sacrifice to determine either cell type distribution or whole organ particle localization. (B) Comparative biodistribution between healthy and neb-LPS challenged mice given aPECAM, DOTAP, and combined LNPs shows enhancement of localization for all formulations to the lung following neb-LPS challenge. Combined LNPs localize to the lungs 3-fold and 2.25-fold more than aPECAM and DOTAP LNPs, respectively, following neb-LPS challenge. (C) Comparison of lung-to-liver ratios between healthy and neb-LPS challenged mice shows significant enhancement to lung localization after neb-LPS challenge for all formulations but especially for the combined formulation, getting an almost 2-fold improvement in lung targeting. Similarly, combined LNPs have a >2-fold higher lung to liver ratio compared to aPECAM or DOTAP LNPs also after neb-LPS injury. (D) Quantification of the effect of pathological lung uptake and delivery aPECAM, DOTAP, and Combined LNP formulations. Dividing the %ID/g of LNP in the lung after neb-LPS by the %ID/g in healthy lung shows that aPECAM, DOTAP, and Combined LNPs increase localization between 1.5 and 2 fold increase in lung localization. (E) Gating first by cell type (endothelial cells) and then identifying the percentage that are LNP positive shows that pathology does not influence uptake of LNPs by endothelial cells. (F) Similarly, this is the case for neutrophils. Statistics: $n = 3$ and data shown represent mean ± SEM. Comparisons between groups were made using 1-way ANOVA or 2-way ANOVA with Tukey's posthoc test where appropriate. *$p < 0.05$, ***$p < 0.001$, ****$p < 0.0001$.

were taken up in monocytes/macrophages at a significantly higher rate than aPECAM LNPs. But uptake in monocytes/macrophages was low, with only 30% of monocytes and macrophages taking up DOTAP and Combined LNPs. Uptake in other leukocytes was similarly low for all of the LNP formulations.

We next investigated the correlation between cell type uptake and expression. To do this, we generated our three LNP formulations loaded with mRNA expressing Cre-recombinase. These LNPs were then injected into the Ai6 Cre reporter mice. Ai6 mice have a loxP-flanked Stop cassette preventing transcription of an enhanced green fluorescent

https://doi.org/10.1021/acs.nanolett.3c05031
Nano Lett. 2024, 24, 4774−4784

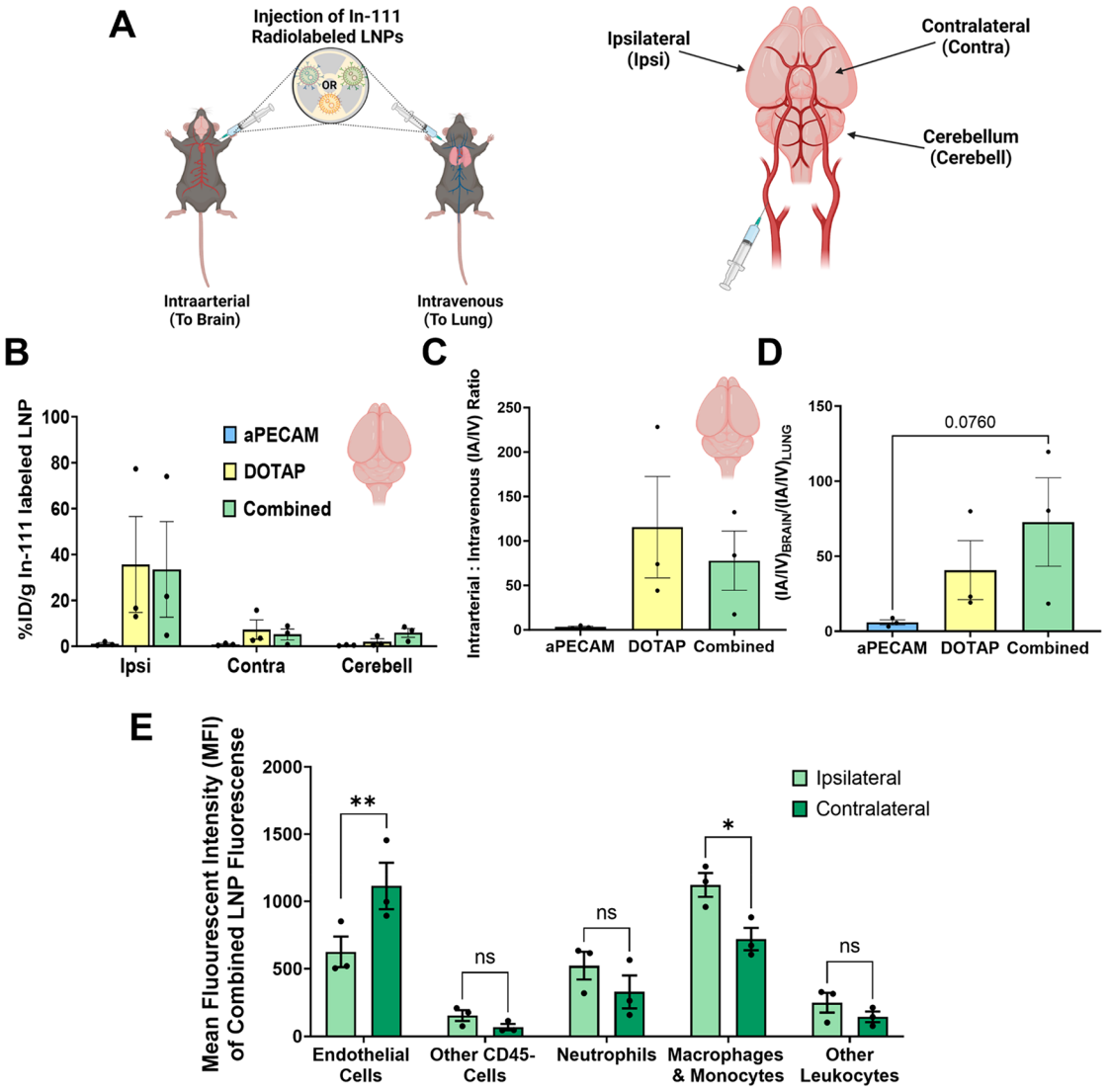

Figure 4. DOTAP and Combined LNP formulations are dependent on first pass privilege for brain localization, but provide unprecedented targeting to the brain. A test for targeted therapeutics specificity to the lung is to measure the dependence of the first pass effect as the lung is the first major capillary bed targeted therapeutics face. (A) To eliminate the first pass effect, In-111 radiolabeled aPECAM, DOTAP, and Combined LNPs were injected intra-arterially (IA) into the right carotid artery and allowed to circulate for 30 min, the animals were then sacrificed and organs measured for radioactivity, this was compared to direct intravenous delivery (IV) via retro orbital injection. Segments of the brain were dissected as shown in (A) (right) identifying the ipsilateral (same side of injection), contralateral (opposing side of injection), and the cerebellum. (B) Following IA injection of aPECAM, DOTAP, and Combined LNPs, we show enhanced localization by DOTAP and Combined LNPs in the brain, specifically in the ipsilateral cerebrum (the same side where the LNP was injected). (C) Directly comparing the %ID/g in the brain after IA injection to %ID/g after IV injection highlights that for brain localization, where IA administration gives the brain capillary bed first pass privilege, enhanced delivery by DOTAP and Combined LNPs by an order of magnitude. (D) We next compare this IA:IV ratio in the brain to that of the lung to better evaluate the intraarterial first pass effect dependence on targeting to the brain. (E) To determine the cell types in the brain that take up Combined LNPs, we injected fluorescently labeled Combined LNPs and separately prepared the ipsilateral and contralateral hemispheres of the brain. In the contralateral side of the brain, LNPs are taken up more by cerebral vascular endothelial cells, whereas LNPs are taken up more by monocytes and macrophages in the ipsilateral side of the brain. Statistics. $n = 3$ and data shown represent mean ± SEM. Comparisons between groups were made using 1-way ANOVA, where appropriate, with Tukey's posthoc test. $^{*}p < 0.05$, $^{***}p < 0.001$.

protein (eGFP), all inserted into the ROSA-26locus as shown in Figure 2F. Using this method, we find that all three formulations drive eGFP expression in endothelial cells but aPECAM and Combined LNPs outcompete DOTAP LNPs for endothelial expression. Interestingly, we also find that these 2 formulations also express in monocytes and macrophages Figure 2G.

We next used the most common model for ARDS, nebulized LPS (neb-LPS),[61,62] to investigate how acute lung inflammation affects LNP lung targeting and cell type specificity. Radiolabeled or fluorescent LNPs were administered IV, 4 h after neb-LPS, after inflammatory processes and neutrophilic infiltration into the lung have developed (Figure 3A).

In radiotracer data, Combined LNPs had a 2-fold improvement in lung uptake in neb-LPS mice vs healthy animals (Figure 3B and Supporting Figure 1). Lung uptake of Combined LNPs in neb-LPS mice was also 2-fold higher than that of aPECAM or DOTAP LNPs. Lung-to-liver uptake ratio follows a similar trend (Figure 3C), showing the high lung specificity of Combined LNPs after neb-LPS injury. We

https://doi.org/10.1021/acs.nanolett.3c05031
Nano Lett. 2024, 24, 4774−4784

define a "pathology ratio" as lung uptake in neb-LPS mice divided by lung uptake in healthy mice. aPECAM, DOTAP, and Combined LNPs had statistically similar pathology ratios, with neb-LPS causing a ∼1.5- to 2-fold increase in lung uptake (Figure 3D).

Despite increased lung uptake in radiotracer data, in flow cytometry, there was no increase in the fraction of either endothelial cells or neutrophils positive for LNPs when comparing neb-LPS to healthy mice (Figure 3E,F). Epithelial and mesenchymal uptake of DOTAP and Combined LNPs was similarly conserved (Supporting Figure 3G). There was an increase in monocyte and macrophage uptake of DOTAP and Combined LNPs, from 30% positive in healthy mice to 50% in neb-LPS mice (Supporting Figure 3B,F). However, the mean LNP fluorescence for these cell types does not increase, suggesting they are not the source for the increase in lung uptake (Supporting Figure 3D).

Since the lungs possess the first capillary bed downstream of an IV injection, we used intraarterial (IA) injection in the right carotid artery to see if a first pass effect may (a) contribute to lung uptake of our LNPs; (b) allow for increased LNP uptake in the brain after intracarotid injection (Figure 4A). After IA injection, radiolabeled aPECAM, DOTAP, and Combined LNPs were allowed to circulate for 30 min before assessing biodistributions.

DOTAP LNPs have increased uptake in the lungs after IA injection, compared to IV injection (Supporting Figure 4A,B). This may be because IA injection provides the DOTAP LNPs an extra cardiac cycle before lung exposure, allowing for accumulation of additional opsonins (see the discussion for further hypotheses). aPECAM and Combined LNPs' lung uptake was unaffected by the injection method. Our results indicate a first-pass effect is not the main reason for lung uptake of our targeted LNPs.

After IA injection in the right carotid artery, we observed a high uptake of DOTAP and Combined LNPs in the brain but no such uptake with aPECAM LNPs. Uptake of DOTAP and Combined LNPs in the right (ipsilateral to injection site) hemisphere was 35% ID/g, which is, to our knowledge, the highest reported delivery to the brain (Figure 4B).[63,64] IA injection moderately increases the DOTAP and Combined LNP uptake in the contralateral side and the cerebellum. Comparing ipsilateral brain uptake of LNPs after IA vs IV delivery shows that IA delivery increases brain delivery ∼50−100-fold (Figure 4C). Implying DOTAP-containing LNP brain uptake is almost entirely first-pass mediated. Comparing the IA-to-IV ratio for brain uptake versus lung uptake shows a greater first-pass effect for brain delivery than for lung delivery of DOTAP-containing LNPs, especially Combined LNPs (Figure 4D).

Last, we tested the cell-type uptake of our Combined LNP following intra-arterial injection (Figure 4E). Following circulation, the brains were separated into ipsilateral and contralateral hemispheres. We found that about 20−40% of the endothelial cells are positive for LNP delivery, which is impressive compared to prior delivery technologies.

Two classes of targeting methods have achieved LNP delivery to specific cell types and organs: affinity moiety targeting[34,36,37,40] and physicochemical tropism.[24,28−30,65] Here, we directly compare these two methods. We focused on targeted delivery to the lungs using aPECAM LNPs to represent affinity moiety targeting and DOTAP LNPs to represent physicochemical tropism. We also incorporated aPECAM and DOTAP in the same LNPs, to achieve a "Combined" targeting LNP.

Focusing on comparing affinity moiety targeting and physicochemical tropism, both strategies produced nearly identical overall lung uptake. Indeed different targeting strategies yield similar lung uptake, nanoparticles targeted via aPECAM, aICAM,[66] the technique of RBC-hitchhiking,[67−69] and physicochemical tropism to marginated neutrophils.[70] Suggesting a saturation value for lung uptake focused on the alveolar capillaries. Combined LNPs overcome this saturation. Comparing cell type selectivity of affinity moiety targeting vs physicochemical tropism, aPECAM LNPs have better endothelial specificity than DOTAP LNPs. Endothelial cells are traditionally the cells of interest in lung targeting. However, DOTAP provides delivery to cells outside of the vasculature, to epithelial and mesenchymal, promising RNA delivery to lung cell types inaccessible with IV agents. Combined LNPs had >2×-higher lung uptake than either aPECAM or DOTAP alone and provided unprecedented delivery to alveolar epithelial cells. They exhibited 2×-higher delivery to inflamed lungs than to healthy lungs. These advantages encourage investigation of Combined LNPs and their mechanisms of uptake, especially in pathology, like pulmonary inflammation.

Combined LNPs required optimization to work. Particularly, the identity and molar ratio of PEG-lipids must be optimized. Our choice was utilizing DSPE-PEG (18 carbons) for aPECAM-LNPs, DMG-PEG (10 carbons) for DOTAP-LNPs, and a half mix of both to generate our Combined LNPs. DSPE with 18 carbons in its acyl chain anchors the lipid to the surface layer more strongly than DMG, which only has 10 carbons.[9] Conversely, DMG desorbs very quickly in serum, allowing serum proteins (e.g., ApoE) to adsorb onto the LNP surface, driving localization (as shown with FDA-approved patisiran). DSPE is used to anchor lipids for affinity moieties (here anti-PECAM antibodies) to keep the lipid-affinity-moiety conjugate on the LNP surface at least long enough for the affinity moiety to reach its target. DMG is the most used lipid for anchoring PEG when physicochemical tropism is desired. For our Combined LNPs, we "thread the needle", achieving a balance of antibody targeting and protein corona guided localization. Indeed, in Supporting Figure 4E,F, we see that changing the PEG ratio from 1.5% DSPE PEG to a ratio of 0.75% DMG PEG and 0.75% DSPE PEG matching the PEG ratio used in our Combined formulation, we observed ablation of aPECAM LNP lung targeting. Likely, half of the LNPs' PEG desorbed quickly, allowing serum proteins, especially complement proteins such as C3, to adsorb onto the LNPs' antibodies.[12,13] Complement C3-coated antibodies are avidly cleared by Kupffer cells, hence, the high liver expression. Thus, changing the PEG-lipid ratios has a very large effect on comparing the various LNPs.

DOTAP and Combined LNPs strongly localize to the brain following intra-arterial injection. They achieve ∼35% ID/g on the side of the brain ipsilateral to the injection site. This level of brain uptake exceeds standard brain targeting methods, including transferrin and VCAM targeting[63,64] and is largely unilateral. This can be useful for brain injuries that present unilaterally, including stroke and traumatic brain injuries.

When targeting the brain, Combined LNPs were mostly taken up by endothelial cells and innate immune cells instead of neurons. While in some applications the goal is to target the neurons, targeting endothelial cells and leukocytes is actually quite advantageous for acute brain injuries, like ischemic

https://doi.org/10.1021/acs.nanolett.3c05031
Nano Lett. 2024, 24, 4774−4784

stroke, hemorrhagic stroke, and traumatic brain injury.[34,63,71−73] Our goal is not to target LNPs past the BBB (blood−brain barrier), but rather to the endothelial cells of the BBB. In all these acute brain injuries, the BBB endothelium is leaky, allowing toxic plasma proteins and innate immune cells to cross the BBB and contact the parenchyma, injuring the neurons. We have shown that targeting LNPs to endothelial cells, delivering anti-inflammatory proteins like IL-10 or thrombomodulin, can seal up the BBB and reduce inflammation and neuronal injury.[63,71] Additionally, targeting LNPs to the neutrophils and monocytes that surround the BBB can ameliorate neuronal inflammation.[34] Thus, targeting the brain endothelial cells, neutrophils, and macrophages is a major goal but is limited by other technologies achieving ∼1% of the injected dose (%ID) to the brain, a tiny fraction going to these cells.

The intracarotid injections of Combined LNPs provides >20× improvement in the %ID in the brain. Therefore, we hoped that it also provided good delivery to endothelial cells, neutrophils, and monocytes, and indeed, the data in Figure 4E and Supporting Figure 7A shows that it does. 20−40% of endothelial cells are positive for LNP delivery, which is impressive compared to prior delivery technologies.

Safety and side effects are critical issues that must be investigated in future studies. Combined LNPs will have side effects, and it is important to investigate these and attempt to engineer solutions. Of greatest concern with DOTAP-containing LNPs is that IV LNPs formulated with any of various cationic lipids cause thrombosis.[74] It is reasonable to hypothesize that Combined LNPs may have similar effects. However, our recent work also demonstrated techniques to mitigate clotting induced by cationic lipid LNPs, including anticoagulation and reduced LNP size. These techniques should be applied to Combined LNPs in future studies. It remains to be seen whether these or other engineered solutions will be sufficient to make the risk-benefit ratio meet the criterion for further preclinical development of what appears to be a promising targeting technology.

Additional safety concerns include LNP-associated inflammation. We have previously shown that LNPs as a class worsen pre-existing inflammation.[75] In this manuscript, we attempted to measure LNP-based mRNA expression after intracarotid artery injection; however, the mice did not survive. Cannulation and injection of the carotid artery in mice is a technically difficult procedure, usually done for 2 h short-term experiments. After many attempts, we were unable to get mice to survive the 4 h found to be necessary to observe significant expression from mRNA LNPs. A big surgery like carotid artery exposure and cannulation induces a major inflammatory response, which is compounded by mRNA-LNPs worsening pre-existing inflammation.[75] Thus, we could not determine the correlation between the delivery and expression in the brain.

However, we successfully correlated mRNA delivery versus expression after intravenous (IV) delivery. First, we showed in Figure 1B−F in the lungs that, for these formulations (aPECAM, DOTAP, Combined), the LNPs' expression and localization correlate very well with one another and can be used as surrogate measures. Additionally, in Figure 2G, we examined the cell-type-specific expression of LNPs in the Ai6 mouse model. Figure 2G shows that the expression data looks like the delivery data, with the exception that neutrophils do not express highly, primarily due to their 6−8-h half-life and we measured expression at 24 h. At the level of whole-organ biodistribution and comparative cell type level, these LNPs appear to have delivery/uptake that correlate well with expression of their cargo mRNA. While we cannot be sure of such a correlation upon intracarotid delivery to the brain, the main point of Figure 4 shows DOTAP provides *first-pass* delivery, indicating localization to the first capillary bed encountered.

DOTAP-containing LNPs have greater uptake by innate immune cells, possibly leading to even greater inflammation in comparison to other LNPs. Flow cytometry data shows that DOTAP and Combined LNPs are avidly taken up by innate immune cells, especially in acute lung injury (Figures 2B and 3F and Supporting Figure 3A,B,F). This increased immune uptake of LNPs increases the potential for activation of inflammatory pathways, possibly allowing later adaptive immunity against the LNPs. Future studies should aim to engineer solutions to uptake of DOTAP-containing LNPs by innate immune cells, such as adding on "don't eat me" signals such as CD47-mimetic peptides.[76] Conversely, DOTAP-LNPs' uptake by innate immune cells also present new targets for RNA delivery and disease-specific treatment.[62,77−79]

■ ASSOCIATED CONTENT

Supporting Information

The Supporting Information is available free of charge at https://pubs.acs.org/doi/10.1021/acs.nanolett.3c05031.

Materials and methods; Size and zeta potential for all formulations; Supporting biodistributions; Cell type gating strategy; Cell markers and fluorophores utilized; Supporting uptake and expression (luciferase and eGFP expression); Cell type distributions (PDF)

■ AUTHOR INFORMATION

Corresponding Authors

Jacob S. Brenner − *University of Pennsylvania, School of Systems Pharmacology and Translational Therapeutics and Department of Bioengineering, Philadelphia, Pennsylvania 19104, United States;* orcid.org/0000-0001-8437-0161; Email: jacob.brenner@pennmedicine.upenn.edu

Jacob W. Myerson − *University of Pennsylvania, School of Systems Pharmacology and Translational Therapeutics, Philadelphia, Pennsylvania 19104, United States;* Email: spragueclegHorn@gmail.com

Oscar A. Marcos-Contreras − *University of Pennsylvania, School of Systems Pharmacology and Translational Therapeutics, Philadelphia, Pennsylvania 19104, United States;* Email: oscarmar@pennmedicine.upenn.edu

Authors

Marco E. Zamora − *Drexel University, School of Biomedical Engineering, Philadelphia, Pennsylvania 19104, United States; University of Pennsylvania, School of Systems Pharmacology and Translational Therapeutics, Philadelphia, Pennsylvania 19104, United States;* orcid.org/0000-0002-7858-307X

Serena Omo-Lamai − *University of Pennsylvania, Department of Bioengineering, Philadelphia, Pennsylvania 19104, United States*

Manthan N. Patel − *University of Pennsylvania, School of Systems Pharmacology and Translational Therapeutics, Philadelphia, Pennsylvania 19104, United States*

https://doi.org/10.1021/acs.nanolett.3c05031
Nano Lett. 2024, 24, 4774−4784

Jichuan Wu − *University of Pennsylvania, School of Systems Pharmacology and Translational Therapeutics, Philadelphia, Pennsylvania 19104, United States*
Evguenia Arguiri − *University of Pennsylvania, School of Systems Pharmacology and Translational Therapeutics, Philadelphia, Pennsylvania 19104, United States*
Vladmir R. Muzykantov − *University of Pennsylvania, School of Systems Pharmacology and Translational Therapeutics, Philadelphia, Pennsylvania 19104, United States*

Complete contact information is available at: https://pubs.acs.org/10.1021/acs.nanolett.3c05031

Author Contributions

#These authors contributed equally to this work (M.E.Z. and S.O.-L.).

Notes

The authors declare no competing financial interest.

REFERENCES

(1) Wilhelm, S.; Tavares, A. J.; Dai, Q.; Ohta, S.; Audet, J.; Dvorak, H. F.; Chan, W. C. W. Analysis of Nanoparticle Delivery to Tumours. *Nature Reviews Materials* **2016**, *1* (5), 1−12.
(2) Poon, W.; Zhang, Y.-N.; Ouyang, B.; Kingston, B. R.; Wu, J. L. Y.; Wilhelm, S.; Chan, W. C. W. Elimination Pathways of Nanoparticles. *ACS Nano* **2019**, *13* (5), 5785−5798.
(3) Bachmaier, K.; Stuart, A.; Singh, A.; Mukhopadhyay, A.; Chakraborty, S.; Hong, Z.; Wang, L.; Tsukasaki, Y.; Maienschein-Cline, M.; Ganesh, B. B.; Kanteti, P.; Rehman, J.; Malik, A. B. Albumin Nanoparticle Endocytosing Subset of Neutrophils for Precision Therapeutic Targeting of Inflammatory Tissue Injury. *ACS Nano* **2022**, *16* (3), 4084−4101.
(4) Ouyang, B.; Poon, W.; Zhang, Y.-N.; Lin, Z. P.; Kingston, B. R.; Tavares, A. J.; Zhang, Y.; Chen, J.; Valic, M. S.; Syed, A. M.; MacMillan, P.; Couture-Senécal, J.; Zheng, G.; Chan, W. C. W. The Dose Threshold for Nanoparticle Tumour Delivery. *Nat. Mater.* **2020**, *19* (12), 1362−1371.
(5) Chen, S.-J.; Sanmiguel, J.; Lock, M.; McMenamin, D.; Draper, C.; Limberis, M. P.; Kassim, S. H.; Somanathan, S.; Bell, P.; Johnston, J. C.; Rader, D. J.; Wilson, J. M. Biodistribution of AAV8 Vectors Expressing Human Low-Density Lipoprotein Receptor in a Mouse Model of Homozygous Familial Hypercholesterolemia. *Hum Gene Ther Clin Dev* **2013**, *24* (4), 154−160.
(6) Torchilin, V. P.; Khaw, B. A.; Smirnov, V. N.; Haber, E. Preservation of Antimyosin Antibody Activity after Covalent Coupling to Liposomes. *Biochem. Biophys. Res. Commun.* **1979**, *89* (4), 1114−1119.
(7) Huang, A.; Kennel, S. J.; Huang, L. Interactions of Immunoliposomes with Target Cells. *J. Biol. Chem.* **1983**, *258* (22), 14034−14040.
(8) Heath, T. D.; Fraley, R. T.; Papahdjopoulos, D. Antibody Targeting of Liposomes: Cell Specificity Obtained by Conjugation of F(ab')2 to Vesicle Surface. *Science* **1980**, *210* (4469), 539−541.
(9) Gregoriadis, G. Homing of Liposomes to Target Cells. *Biochem. Soc. Trans.* **1975**, *3* (5), 613−618.
(10) Gregoriadis, G. Targeting of Drugs. *Nature* **1977**, *265* (5593), 407−411.
(11) Magee, W. E.; Miller, O. V. Liposomes Containing Antiviral Antibody Can Protect Cells from Virus Infection. *Nature* **1972**, *235* (5337), 339−341.
(12) Kułdo, J. M.; Ogawara, K. I.; Werner, N.; Asgeirsdóttir, S. A.; Kamps, J. A. A. M.; Kok, R. J.; Molema, G. Molecular Pathways of Endothelial Cell Activation for (targeted) Pharmacological Intervention of Chronic Inflammatory Diseases. *Curr. Vasc. Pharmacol.* **2005**, *3* (1), 11−39.
(13) Ahmad, I.; Arsalan, A.; Ali, S. A.; Sheraz, M. A.; Ahmed, S.; Anwar, Z.; Munir, I.; Shah, M. R. Formulation and Stabilization of Riboflavin in Liposomal Preparations. *J. Photochem. Photobiol., B* **2015**, *153*, 358−366.
(14) Suntres, Z. E.; Shek, P. N. Prophylaxis against Lipopolysaccharide-Induced Acute Lung Injury by Alpha-Tocopherol Liposomes. *Crit. Care Med.* **1998**, *26* (4), 723−729.
(15) Yamakawa, T.; Ohigashi, H.; Hashimoto, D.; Hayase, E.; Takahashi, S.; Miyazaki, M.; Minomi, K.; Onozawa, M.; Niitsu, Y.; Teshima, T. Vitamin A-Coupled Liposomes Containing siRNA against HSP47 Ameliorate Skin Fibrosis in Chronic Graft-versus-Host Disease. *Blood* **2018**, *131* (13), 1476−1485.
(16) Khan, A. A.; Allemailem, K. S.; Almatroodi, S. A.; Almatroudi, A.; Rahmani, A. H. Recent Strategies towards the Surface Modification of Liposomes: An Innovative Approach for Different Clinical Applications. *3 Biotech* **2020**, *10* (4), 163.
(17) Xu, L.; Huang, C.-C.; Huang, W.; Tang, W.-H.; Rait, A.; Yin, Y. Z.; Cruz, I.; Xiang, L.-M.; Pirollo, K. F.; Chang, E. H. Systemic Tumor-Targeted Gene Delivery by Anti-Transferrin Receptor scFv-Immunoliposomes. *Mol. Cancer Ther.* **2002**, *1* (5), 337−346.
(18) Mamot, C.; Drummond, D. C.; Hong, K.; Kirpotin, D. B.; Park, J. W. Liposome-Based Approaches to Overcome Anticancer Drug Resistance. *Drug Resist. Updat.* **2003**, *6* (5), 271−279.
(19) Miller, K.; Cortes, J.; Hurvitz, S. A.; Krop, I. E.; Tripathy, D.; Verma, S.; Riahi, K.; Reynolds, J. G.; Wickham, T. J.; Molnar, I.; Yardley, D. A. HERMIONE: A Randomized Phase 2 Trial of MM-302 plus Trastuzumab versus Chemotherapy of Physician's Choice plus Trastuzumab in Patients with Previously Treated, Anthracycline-Naïve, HER2-Positive, Locally Advanced/metastatic Breast Cancer. *BMC Cancer* **2016**, *16*, 352.
(20) Xie, F.; Xie, F.; Qin; Yuan; Tang; Zhang; Fan; Chen; Hai; Yao; Li; He, Q. Investigation of Glucose-Modified Liposomes Using Polyethylene Glycols with Different Chain Lengths as the Linkers for Brain Targeting. *Int. J. Nanomedicine* **2012**, *7*, 163−175.
(21) Abu-Dahab, R.; Schäfer, U. F.; Lehr, C. M. Lectin-Functionalized Liposomes for Pulmonary Drug Delivery: Effect of Nebulization on Stability and Bioadhesion. *Eur. J. Pharm. Sci.* **2001**, *14* (1), 37−46.
(22) Anselmo, A. C.; Mitragotri, S. Nanoparticles in the Clinic. *Bioeng Transl Med.* **2016**, *1* (1), 10−29.
(23) Anselmo, A. C.; Mitragotri, S. Nanoparticles in the Clinic: An Update. *Bioeng. Transl. Med.* **2019**, *4* (3), e10143.
(24) Siegwart, D. J.; Whitehead, K. A.; Nuhn, L.; Sahay, G.; Cheng, H.; Jiang, S.; Ma, M.; Lytton-Jean, A.; Vegas, A.; Fenton, P.; Levins, C. G.; Love, K. T.; Lee, H.; Cortez, C.; Collins, S. P.; Li, Y. F.; Jang, J.; Querbes, W.; Zurenko, C.; Novobrantseva, T.; Langer, R.; Anderson, D. G. Combinatorial Synthesis of Chemically Diverse Core-Shell Nanoparticles for Intracellular Delivery. *Proc. Natl. Acad. Sci. U. S. A.* **2011**, *108* (32), 12996−13001.
(25) Lee, H.; Lytton-Jean, A. K. R.; Chen, Y.; Love, K. T.; Park, A. I.; Karagiannis, E. D.; Sehgal, A.; Querbes, W.; Zurenko, C. S.; Jayaraman, M.; Peng, C. G.; Charisse, K.; Borodovsky, A.; Manoharan, M.; Donahoe, J. S.; Truelove, J.; Nahrendorf, M.; Langer, R.; Anderson, D. G. Molecularly Self-Assembled Nucleic Acid Nanoparticles for Targeted in Vivo siRNA Delivery. *Nat. Nanotechnol.* **2012**, *7* (6), 389−393.
(26) Love, K. T.; Mahon, K. P.; Levins, C. G.; Whitehead, K. A.; Querbes, W.; Dorkin, J. R.; Qin, J.; Cantley, W.; Qin, L. L.; Racie, T.; Frank-Kamenetsky, M.; Yip, K. N.; Alvarez, R.; Sah, D. W. Y.; de Fougerolles, A.; Fitzgerald, K.; Koteliansky, V.; Akinc, A.; Langer, R.; Anderson, D. G. Lipid-like Materials for Low-Dose, in Vivo Gene Silencing. *Proc. Natl. Acad. Sci. U. S. A.* **2010**, *107* (5), 1864−1869.
(27) Akinc, A.; Zumbuehl, A.; Goldberg, M.; Leshchiner, E. S.; Busini, V.; Hossain, N.; Bacallado, S. A.; Nguyen, D. N.; Fuller, J.; Alvarez, R.; Borodovsky, A.; Borland, T.; Constien, R.; de Fougerolles, A.; Dorkin, J. R.; Narayanannair Jayaprakash, K.; Jayaraman, M.; John, M.; Koteliansky, V.; Manoharan, M.; Nechev, L.; Qin, J.; Racie, T.; Raitcheva, D.; Rajeev, K. G.; Sah, D. W. Y.; Soutschek, J.; Toudjarska, I.; Vornlocher, H.-P.; Zimmermann, T. S.; Langer, R.; Anderson, D. G. A Combinatorial Library of Lipid-like Materials for Delivery of RNAi Therapeutics. *Nat. Biotechnol.* **2008**, *26* (5), 561−569.

(28) Cheng, Q.; Wei, T.; Farbiak, L.; Johnson, L. T.; Dilliard, S. A.; Siegwart, D. J. Selective Organ Targeting (SORT) Nanoparticles for Tissue-Specific mRNA Delivery and CRISPR-Cas Gene Editing. *Nat. Nanotechnol.* **2020**, *15* (4), 313−320.
(29) Wang, X.; Liu, S.; Sun, Y.; Yu, X.; Lee, S. M.; Cheng, Q.; Wei, T.; Gong, J.; Robinson, J.; Zhang, D.; Lian, X.; Basak, P.; Siegwart, D. J. Preparation of Selective Organ-Targeting (SORT) Lipid Nanoparticles (LNPs) Using Multiple Technical Methods for Tissue-Specific mRNA Delivery. *Nat. Protoc.* **2023**, *18*, 265.
(30) LoPresti, S. T.; Arral, M. L.; Chaudhary, N.; Whitehead, K. A. The Replacement of Helper Lipids with Charged Alternatives in Lipid Nanoparticles Facilities Targeted mRNA Delivery to the Spleen and Lungs. *J. Controlled Release* **2022**, *345*, 819.
(31) Billingsley, M. M.; Singh, N.; Ravikumar, P.; Zhang, R.; June, C. H.; Mitchell, M. J. Ionizable Lipid Nanoparticle-Mediated mRNA Delivery for Human CAR T Cell Engineering. *Nano Lett.* **2020**, *20* (3), 1578−1589.
(32) Billingsley, M. M.; Hamilton, A. G.; Mai, D.; Patel, S. K.; Swingle, K. L.; Sheppard, N. C.; June, C. H.; Mitchell, M. J. Orthogonal Design of Experiments for Optimization of Lipid Nanoparticles for mRNA Engineering of CAR T Cells. *Nano Lett.* **2022**, *22* (1), 533−542.
(33) Adams, D.; Suhr, O. B.; Dyck, P. J.; Litchy, W. J.; Leahy, R. G.; Chen, J.; Gollob, J.; Coelho, T. Trial Design and Rationale for APOLLO, a Phase 3, Placebo-Controlled Study of Patisiran in Patients with Hereditary ATTR Amyloidosis with Polyneuropathy. *BMC Neurol.* **2017**, *17* (1), 181.
(34) Nong, J.; Glassman, P. M.; Myerson, J. W.; Zuluaga-Ramirez, V.; Rodriguez-Garcia, A.; Mukalel, A.; Omo-Lamai, S.; Walsh, L. R.; Zamora, M. E.; Gong, X.; Wang, Z.; Bhamidipati, K.; Kiseleva, R. Y.; Villa, C. H.; Greineder, C. F.; Kasner, S. E.; Weissman, D.; Mitchell, M. J.; Muro, S.; Persidsky, Y.; Brenner, J. S.; Muzykantov, V. R.; Marcos-Contreras, O. A. Targeted Nanocarriers Co-Opting Pulmonary Intravascular Leukocytes for Drug Delivery to the Injured Brain. *ACS Nano* **2023**, *17*, 13121.
(35) Paris, A. J.; Guo, L.; Dai, N.; Katzen, J. B.; Patel, P. N.; Worthen, G. S.; Brenner, J. S. Using Selective Lung Injury to Improve Murine Models of Spatially Heterogeneous Lung Diseases. *PLoS One* **2019**, *14* (4), No. e0202456.
(36) Parhiz, H.; Shuvaev, V. V.; Pardi, N.; Khoshnejad, M.; Kiseleva, R. Y.; Brenner, J. S.; Uhler, T.; Tuyishime, S.; Mui, B. L.; Tam, Y. K.; Madden, T. D.; Hope, M. J.; Weissman, D.; Muzykantov, V. R. PECAM-1 Directed Re-Targeting of Exogenous mRNA Providing Two Orders of Magnitude Enhancement of Vascular Delivery and Expression in Lungs Independent of Apolipoprotein E-Mediated Uptake. *J. Controlled Release* **2018**, *291*, 106−115.
(37) Glassman, P. M.; Myerson, J. W.; Ferguson, L. T.; Kiseleva, R. Y.; Shuvaev, V. V.; Brenner, J. S.; Muzykantov, V. R. Targeting Drug Delivery in the Vascular System: Focus on Endothelium. *Adv. Drug Delivery Rev.* **2020**, *157*, 96−117.
(38) Reyes-Esteves, S.; Nong, J.; Glassman, P. M.; Omo-Lamai, S.; Ohashi, S.; Myerson, J. W.; Zamora, M. E.; Ma, X.; Kasner, S. E.; Sansing, L.; Muzykantov, V. R.; Marcos-Contreras, O. A.; Brenner, J. S. Targeted Drug Delivery to the Brain Endothelium Dominates over Passive Delivery via Vascular Leak in Experimental Intracerebral Hemorrhage. *J. Controlled Release* **2023**, *356*, 185−195.
(39) Muro, S.; Garnacho, C.; Champion, J. A.; Leferovich, J.; Gajewski, C.; Schuchman, E. H.; Mitragotri, S.; Muzykantov, V. R. Control of Endothelial Targeting and Intracellular Delivery of Therapeutic Enzymes by Modulating the Size and Shape of ICAM-1-Targeted Carriers. *Mol. Ther.* **2008**, *16* (8), 1450−1458.
(40) Hood, E. D.; Greineder, C. F.; Shuvaeva, T.; Walsh, L.; Villa, C. H.; Muzykantov, V. R. Vascular Targeting of Radiolabeled Liposomes with Bio-Orthogonally Conjugated Ligands: Single Chain Fragments Provide Higher Specificity than Antibodies. *Bioconjugate Chem.* **2018**, *29* (11), 3626−3637.
(41) Shuvaev, V. V.; Muro, S.; Arguiri, E.; Khoshnejad, M.; Tliba, S.; Christofidou-Solomidou, M.; Muzykantov, V. R. Size and Targeting to PECAM vs ICAM Control Endothelial Delivery, Internalization and Protective Effect of Multimolecular SOD Conjugates. *J. Controlled Release* **2016**, *234*, 115−123.
(42) Manthe, R. L.; Muro, S. ICAM-1-Targeted Nanocarriers Attenuate Endothelial Release of Soluble ICAM-1, an Inflammatory Regulator. *Bioeng Transl Med.* **2017**, *2* (1), 109−119.
(43) Han, J.; Zern, B. J.; Shuvaev, V. V.; Davies, P. F.; Muro, S.; Muzykantov, V. Acute and Chronic Shear Stress Differently Regulate Endothelial Internalization of Nanocarriers Targeted to Platelet-Endothelial Cell Adhesion Molecule-1. *ACS Nano* **2012**, *6* (10), 8824−8836.
(44) McIntosh, D. P.; Tan, X.-Y.; Oh, P.; Schnitzer, J. E. Targeting Endothelium and Its Dynamic Caveolae for Tissue-Specific Transcytosis in Vivo: A Pathway to Overcome Cell Barriers to Drug and Gene Delivery. *Proc. Natl. Acad. Sci. U. S. A.* **2002**, *99* (4), 1996−2001.
(45) Ireson, C. R.; Kelland, L. R. Discovery and Development of Anticancer Aptamers. *Mol. Cancer Ther.* **2006**, *5* (12), 2957−2962.
(46) Santos, M. L. d.; Quintilio, W.; Manieri, T. M.; Tsuruta, L. R.; Moro, A. M. Advances and Challenges in Therapeutic Monoclonal Antibodies Drug Development. *Braz. J. Pharm. Sci.* **2018**, *54* (spe), No. e01007.
(47) Deng, Z.; Kalin, G. T.; Shi, D.; Kalinichenko, V. V. Nanoparticle Delivery Systems with Cell-Specific Targeting for Pulmonary Diseases. *Am. J. Respir. Cell Mol. Biol.* **2021**, *64* (3), 292−307.
(48) Arthur, R. CordenPharma increases xRNA-based capabilities with LNP formulation investment in Italy. https://www.biopharma-reporter.com/Article/2022/06/02/CordenPharma-increases-xRNA-based-capabilities-with-LNP-formulation-investment-in-Italy (accessed 2023−11−01).
(49) Verma, M.; Ozer, I.; Xie, W.; Gallagher, R.; Teixeira, A.; Choy, M. The Landscape for Lipid-Nanoparticle-Based Genomic Medicines. *Nat. Rev. Drug Discovery* **2023**, *22* (5), 349−350.
(50) Oud, L.; Garza, J. The Contribution of COVID-19 to Acute Respiratory Distress Syndrome-Related Mortality in the United States. *J. Clin. Med. Res.* **2023**, *15* (5), 279−281.
(51) Matthay, M. A.; Ware, L. B.; Zimmerman, G. A. The Acute Respiratory Distress Syndrome. *J. Clin. Invest.* **2012**, *122* (8), 2731−2740.
(52) Ware, L. B.; Matthay, M. A. The Acute Respiratory Distress Syndrome. *N. Engl. J. Med.* **2000**, *342* (18), 1334−1349.
(53) Máca, J.; Jor, O.; Holub, M.; Sklienka, P.; Burša, F.; Burda, M.; Janout, V.; Ševčík, P. Past and Present ARDS Mortality Rates: A Systematic Review. *Respir. Care* **2017**, *62* (1), 113−122.
(54) Hasan, S. S.; Capstick, T.; Ahmed, R.; Kow, C. S.; Mazhar, F.; Merchant, H. A.; Zaidi, S. T. R. Mortality in COVID-19 Patients with Acute Respiratory Distress Syndrome and Corticosteroids Use: A Systematic Review and Meta-Analysis. *Expert Rev. Respir. Med.* **2020**, *14* (11), 1149−1163.
(55) Silva, P. L.; Pelosi, P.; Rocco, P. R. M. Personalized Pharmacological Therapy for ARDS: A Light at the End of the Tunnel. *Expert Opin. Investig. Drugs* **2020**, *29* (1), 49−61.
(56) Qiu, M.; Tang, Y.; Chen, J.; Muriph, R.; Ye, Z.; Huang, C.; Evans, J.; Henske, E. P.; Xu, Q. Lung-Selective mRNA Delivery of Synthetic Lipid Nanoparticles for the Treatment of Pulmonary Lymphangioleiomyomatosis. *Proc. Natl. Acad. Sci. U. S. A.* **2022**, *119* (8), na DOI: 10.1073/pnas.2116271119.
(57) Dilliard, S. A.; Sun, Y.; Brown, M. O.; Sung, Y.-C.; Chatterjee, S.; Farbiak, L.; Vaidya, A.; Lian, X.; Wang, X.; Lemoff, A.; Siegwart, D. J. The Interplay of Quaternary Ammonium Lipid Structure and Protein Corona on Lung-Specific mRNA Delivery by Selective Organ Targeting (SORT) Nanoparticles. *J. Controlled Release* **2023**, *361*, 361−372.
(58) Melamed, J. R.; Hajj, K. A.; Chaudhary, N.; Strelkova, D.; Arral, M. L.; Pardi, N.; Alameh, M.-G.; Miller, J. B.; Farbiak, L.; Siegwart, D. J.; Weissman, D.; Whitehead, K. A. Lipid Nanoparticle Chemistry Determines How Nucleoside Base Modifications Alter mRNA Delivery. *J. Controlled Release* **2022**, *341*, 206.

https://doi.org/10.1021/acs.nanolett.3c05031
Nano Lett. 2024, 24, 4774−4784

(59) Hatit, M. Z. C.; Lokugamage, M. P.; Dobrowolski, C. N.; Paunovska, K.; Ni, H.; Zhao, K.; Vanover, D.; Beyersdorf, J.; Peck, H. E.; Loughrey, D.; Sato, M.; Cristian, A.; Santangelo, P. J.; Dahlman, J. E. Species-Dependent in Vivo mRNA Delivery and Cellular Responses to Nanoparticles. *Nat. Nanotechnol.* **2022**, *17* (3), 310−318.
(60) Miao, L.; Lin, J.; Huang, Y.; Li, L.; Delcassian, D.; Ge, Y.; Shi, Y.; Anderson, D. G. Synergistic Lipid Compositions for Albumin Receptor Mediated Delivery of mRNA to the Liver. *Nat. Commun.* **2020**, *11* (1), 2424.
(61) de Souza Xavier Costa, N.; Ribeiro Júnior, G.; Dos Santos Alemany, A. A.; Belotti, L.; Zati, D. H.; Frota Cavalcante, M.; Matera Veras, M.; Ribeiro, S.; Kallás, E. G.; Nascimento Saldiva, P. H.; Dolhnikoff, M.; Ferraz da Silva, L. F. Early and Late Pulmonary Effects of Nebulized LPS in Mice: An Acute Lung Injury Model. *PLoS One* **2017**, *12* (9), No. e0185474.
(62) Tsikis, S. T.; Fligor, S. C.; Hirsch, T. I.; Pan, A.; Yu, L. J.; Kishikawa, H.; Joiner, M. M.; Mitchell, P. D.; Puder, M. Lipopolysaccharide-Induced Murine Lung Injury Results in Long-Term Pulmonary Changes and Downregulation of Angiogenic Pathways. *Sci. Rep.* **2022**, *12* (1), 1−12.
(63) Marcos-Contreras, O. A.; Greineder, C. F.; Kiseleva, R. Y.; Parhiz, H.; Walsh, L. R.; Zuluaga-Ramirez, V.; Myerson, J. W.; Hood, E. D.; Villa, C. H.; Tombacz, I.; Pardi, N.; Seliga, A.; Mui, B. L.; Tam, Y. K.; Glassman, P. M.; Shuvaev, V. V.; Nong, J.; Brenner, J. S.; Khoshnejad, M.; Madden, T.; Weissmann, D.; Persidsky, Y.; Muzykantov, V. R. Selective Targeting of Nanomedicine to Inflamed Cerebral Vasculature to Enhance the Blood-Brain Barrier. *Proc. Natl. Acad. Sci. U. S. A.* **2020**, *117* (7), 3405−3414.
(64) Thomsen, M. S.; Johnsen, K. B.; Kucharz, K.; Lauritzen, M.; Moos, T. Blood-Brain Barrier Transport of Transferrin Receptor-Targeted Nanoparticles. *Pharmaceutics* **2022**, *14* (10), 2237.
(65) Sago, C. D.; Lokugamage, M. P.; Paunovska, K.; Vanover, D. A.; Monaco, C. M.; Shah, N. N.; Gamboa Castro, M.; Anderson, S. E.; Rudoltz, T. G.; Lando, G. N.; Munnilal Tiwari, P.; Kirschman, J. L.; Willett, N.; Jang, Y. C.; Santangelo, P. J.; Bryksin, A. V.; Dahlman, J. E. High-Throughput in Vivo Screen of Functional mRNA Delivery Identifies Nanoparticles for Endothelial Cell Gene Editing. *Proc. Natl. Acad. Sci. U. S. A.* **2018**, *115* (42), E9944−E9952.
(66) Brenner, J. S.; Bhamidipati, K.; Glassman, P. M.; Ramakrishnan, N.; Jiang, D.; Paris, A. J.; Myerson, J. W.; Pan, D. C.; Shuvaev, V. V.; Villa, C. H.; Hood, E. D.; Kiseleva, R.; Greineder, C. F.; Radhakrishnan, R.; Muzykantov, V. R. Mechanisms That Determine Nanocarrier Targeting to Healthy versus Inflamed Lung Regions. *Nanomedicine* **2017**, *13* (4), 1495−1506.
(67) Brenner, J. S.; Mitragotri, S.; Muzykantov, V. R. Red Blood Cell Hitchhiking: A Novel Approach for Vascular Delivery of Nanocarriers. *Annu. Rev. Biomed. Eng.* **2021**, *23*, 225−248.
(68) Ferguson, L. T.; Hood, E. D.; Shuvaeva, T.; Shuvaev, V. V.; Basil, M. C.; Wang, Z.; Nong, J.; Ma, X.; Wu, J.; Myerson, J. W.; Marcos-Contreras, O. A.; Katzen, J.; Carl, J. M.; Morrisey, E. E.; Cantu, E.; Villa, C. H.; Mitragotri, S.; Muzykantov, V. R.; Brenner, J. S. Dual Affinity to RBCs and Target Cells (DART) Enhances Both Organ- and Cell Type-Targeting of Intravascular Nanocarriers. *ACS Nano* **2022**, *16* (3), 4666−4683.
(69) Brenner, J. S.; Pan, D. C.; Myerson, J. W.; Marcos-Contreras, O. A.; Villa, C. H.; Patel, P.; Hekierski, H.; Chatterjee, S.; Tao, J.-Q.; Parhiz, H.; et al. Red Blood Cell-Hitchhiking Boosts Delivery of Nanocarriers to Chosen Organs by Orders of Magnitude. *Nat. Commun.* **2018**, *9* (1), 1−14.
(70) Myerson, J. W.; Patel, P. N.; Rubey, K. M.; Zamora, M. E.; Zaleski, M. H.; Habibi, N.; Walsh, L. R.; Lee, Y.-W.; Luther, D. C.; Ferguson, L. T.; Marcos-Contreras, O. A.; Glassman, P. M.; Mazaleuskaya, L. L.; Johnston, I.; Hood, E. D.; Shuvaeva, T.; Wu, J.; Zhang, H.-Y.; Gregory, J. V.; Kiseleva, R. Y.; Nong, J.; Grosser, T.; Greineder, C. F.; Mitragotri, S.; Worthen, G. S.; Rotello, V. M.; Lahann, J.; Muzykantov, V. R.; Brenner, J. S. Supramolecular Arrangement of Protein in Nanoparticle Structures Predicts Nanoparticle Tropism for Neutrophils in Acute Lung Inflammation. *Nat. Nanotechnol.* **2022**, *17* (1), 86−97.
(71) Nong, J.; Glassman, P. M.; Shuvaev, V. V.; Reyes-Esteves, S.; Descamps, H. C.; Kiseleva, R. Y.; Papp, T. E.; Alameh, M.-G.; Tam, Y. K.; Mui, B. L.; Omo-Lamai, S.; Zamora, M. E.; Shuvaeva, T.; Arguiri, E.; Gong, X.; Brysgel, T. V.; Tan, A. W.; Woolfork, A. G.; Weljie, A.; Thaiss, C. A.; Myerson, J. W.; Weissman, D.; Kasner, S. E.; Parhiz, H.; Muzykantov, V. R.; Brenner, J. S.; Marcos-Contreras, O. A. Targeting Lipid Nanoparticles to the Blood Brain Barrier to Ameliorate Acute Ischemic Stroke. *Mol. Ther.* **2024**, na DOI: 10.1016/j.ymthe.2024.03.004.
(72) Nong, J.; Glassman, P. M.; Muzykantov, V. R. Targeting Vascular Inflammation through Emerging Methods and Drug Carriers. *Adv. Drug Delivery Rev.* **2022**, *184*, 114180.
(73) Marcos-Contreras, O. A.; Brenner, J. S.; Kiseleva, R. Y.; Zuluaga-Ramirez, V.; Greineder, C. F.; Villa, C. H.; Hood, E. D.; Myerson, J. W.; Muro, S.; Persidsky, Y.; Muzykantov, V. R. Combining Vascular Targeting and the Local First Pass Provides 100-Fold Higher Uptake of ICAM-1-Targeted vs Untargeted Nanocarriers in the Inflamed Brain. *J. Controlled Release* **2019**, *301*, 54−61.
(74) Omo-Lamai, S.; Zamora, M. E.; Patel, M. N.; Wu, J.; Nong, J.; Wang, Z.; Peshkova, A.; Majumder, A.; Melamed, J. R.; Chase, L. S.; Essien, E.-O.; Weissman, D.; Muzykantov, V. R.; Marcos-Contreras, O. A.; Myerson, J. W.; Brenner, J. S. Physicochemical Targeting of Lipid Nanoparticles to the Lungs Induces Clotting: Mechanisms and Solutions. *Adv. Mater.* **2024**, e2312026.
(75) Parhiz, H.; Brenner, J. S.; Patel, P. N.; Papp, T. E.; Shahnawaz, H.; Li, Q.; Shi, R.; Zamora, M. E.; Yadegari, A.; Marcos-Contreras, O. A.; Natesan, A.; Pardi, N.; Shuvaev, V. V.; Kiseleva, R.; Myerson, J. W.; Uhler, T.; Riley, R. S.; Han, X.; Mitchell, M. J.; Lam, K.; Heyes, J.; Weissman, D.; Muzykantov, V. R. Added to Pre-Existing Inflammation, mRNA-Lipid Nanoparticles Induce Inflammation Exacerbation (IE). *J. Controlled Release* **2022**, *344*, 50−61.
(76) Rodriguez, P. L.; Harada, T.; Christian, D. A.; Pantano, D. A.; Tsai, R. K.; Discher, D. E. Minimal "Self" Peptides That Inhibit Phagocytic Clearance and Enhance Delivery of Nanoparticles. *Science* **2013**, *339* (6122), 971−975.
(77) Huang, X.; Xiu, H.; Zhang, S.; Zhang, G. The Role of Macrophages in the Pathogenesis of ALI/ARDS. *Mediators Inflamm.* **2018**, *2018*, 1264913.
(78) Dang, W.; Tao, Y.; Xu, X.; Zhao, H.; Zou, L.; Li, Y. The Role of Lung Macrophages in Acute Respiratory Distress Syndrome. *Inflamm. Res.* **2022**, *71* (12), 1417−1432.
(79) Lomas-Neira, J. L.; Heffernan, D. S.; Ayala, A.; Monaghan, S. F. Blockade of Endothelial Growth Factor, Angiopoietin-2, Reduces Indices of ARDS and Mortality in Mice Resulting from the Dual-Insults of Hemorrhagic Shock and Sepsis. *Shock* **2016**, *45* (2), 157−165.

https://doi.org/10.1021/acs.nanolett.3c05031
Nano Lett. 2024, 24, 4774−4784